J Ther Eng, Vol. 8, No. 2, pp. 235–248, March 2022

Journal of Thermal Engineering
Web page info: https://jten.yildiz.edu.tr
DOI: 10.18186/thermal.1086202

Journal of Thermal Engineering

Research Article

Heat transfer investigation of non-newtonian fluid flow in anannular pipe embedded with porous discs: A turbulent study

Zohreh POURSHARIF[1], Hesamoddin SALARIAN[1,*], Kourosh JAVAHERDEH[2], Majid Eshagh NIMVARI[3]

[1]Department of Mechanical Engineering, Nour Branch, Islamic Azad University, Nour, Iran
[2]Faculty of Mechanical Engineering, University of Guilan, Rasht, Iran
[3]Faculty of Engineering, Amol University of Special Modern Technologies, Amol, Iran

ARTICLE INFO

Article history
Received: 15 May 2020
Accepted: 4 November 2020

Keywords:
Non-Newtonian Fluid, Turbulent Flow, Nusselt Number, Annular Pipe, Porous Medium

ABSTRACT

Porous materials are used in thermal devices such as heat exchangers to improvement the heat transfer. The heat transfer of a non-Newtonian fluid flow in an annular pipe with porous discs is numerically investigated in this paper. The flow regime in both porous medium and clear region are considered to be turbulent. The effects of power-law index of the non-Newtonian fluid and porous discs pitch variationson the heat transfer rate, friction coefficient are studied and compared to each other for two porous layer thicknesses. Finally, the thermal performance is defined which determines the optimum porous media and non-Newtonian fluid characteristics in the annular pipe.

Cite this article as: Zohreh P, Hesamoddin S, Kourosh J, Majid E N. Heat transfer investigation of non-newtonian fluid flow in anannular pipe embedded with porous discs: A turbulent study. J Ther Eng 2022;8(2):235–248.

INTRODUCTION

The improvement of heat transfer in double pipe heat exchangers, annular pipes, and pipes has always received attention from researchers. Several techniques have been developed since 1970 to improve the convection heat transfer in annular ducts. Apart from conventional methods to increase the heat transfer inside a duct such as fins and extended surfaces, using a porous medium has become as an interesting method to increase heat transfer in recent years. Generally, metal foams with high porosity percentage (85%-95%) are used for thermal systems. The presence of porous media in numerous engineering applications and natural processes such as ceramic processing, filtration, geothermal systems, groundwater flow, enhanced oil

***Corresponding author.**
*E-mail address: h_salarian@iaunour.ac.ir

This paper was recommended for publication in revised form by Regional Editor Baha Zafer

Published by Yıldız Technical University Press, Istanbul, Turkey

recovery, compact heat exchangers, packed bed chemical reactors and many others. The use of porous/fluid composite systems is an innovative method able to provide valuable solutions for improving energy the efficiency of thermal systems. This can have a positive impact in areas ranging from preservation of energy resources to limiting global warming[1, 2].

The porous medium built with high porosity metal foams increases the heat transfer rate due to their unique properties. The convective heat transfer coefficient is higher for systems filled with porous material than the systems without porous material due to the high thermal conductivity of the porous matrix compared to thermal conductivity, for fluid flows[3], while the working fluid flows through the porous media, it is heated or cooled by the interaction of the porous walls. The advantage of the porous media as the heat exchanger is its wide contact area to the working fluid. Furthermore, due to its tortuous shape the heat transfer is enhanced. The employment of porous media leads to a great increase in heat transfer rate; however, due to the structural features of the porous media, its employment also enlarges the contact area between the porous media and the fluid flow at the same time, thus increases the flow resistance significantly[4]. In addition partially porous media effect on the heat transfer rate. Channeling effect is occurred due to partially porous media that changes velocity distribution and leads to thinner boundary layer on the side that doesn't have porous media.

The flow regime inside the porous layer has been considered to be laminar in most studies[5, 6]. while it has been observed to be turbulent in real applications such as heat exchangers and reactors[7]. This fact maderesearchers investigate the effects of turbulence on the fluid flow and heat transfer in channels partially filled with a porous material. Researchers such as Allouache and Chikh[8] and Nimvari et al.[9] examined the characteristics of flow and heat transfer of a turbulent flow in a region partially filled with a porous material. Allouache and Chikh[8] investigated the turbulent flow in an annular pipe partially filled with a porous material. They utilized a modified $k - \varepsilon$ model to simulate the fluid flow in porous media by time averaging of macroscopic transport equations. They demonstrated that the turbulence intensity is highly affected by porous media permeability and has the maximum value at a certain Darcy number. Mahmoudi and Karimi[10] investigated the heat transfer in a pipe with porous material under the local thermal non-equilibrium condition at the pipe wall. They used Darcy-Brinkman- Forchheimer model to study the fluid in the porous material. These researchers proposed an optimum thickness for the porous material in order to increase the heat transfer at various inertia coefficients for a reasonable pressure loss. Jamarani et al.[11] simulated the fluid flow and the heat transfer in a double pipe heat exchanger partially filled with a porous material using Darcy-Forchheimer equations and local thermal equilibrium. They used two different configurations for the porous layer. In one configuration the porous layer was far from the heat transfer surface and in the other one the porous layer was in contact with heat transfer surface. The results showed that the maximum thermal performance for the first and second cases were S = 0.7 and S = 0.4, respectively (S is the dimensionless area of the porous layer).

Various industries that employ porous medium may face on-Newtonian behavior of the working fluid. Filtration, enhanced oil recovery, chromatography and material analysis are some of the examples. Chen and Hadim[12] studied the forced convection heat transfer of non-Newtonian fluid flow in a duct filled with porous material using numerical methods. They found that a reduction in the power-law index leads to an increase in the heat transfer rate in a non-Darcy flow. Nebly and Bohadef[13] numerically investigated the forced convection heat transfer of the laminar flow of a non-Newtonian fluid in a 3D square duct partially filled with porous material. Their results showed that pseudo plastic fluids have the highest heat transfer rate and pressure loss. Yilmaz et al. [14] conducted some experiments on Newtonian and non-Newtonian fluids in a porous medium. Their purpose was to compare the flow properties (e.g. pressure loss, flow rate, and permeability) of the laminar flow of Newtonian and non-Newtonian viscous elastic fluids within a porous medium. Chen and Tesso[15] studied the convection heat transfer of a laminar flow of a non-Newtonian fluid, power-law model, inside a duct in which porous material was inserted between parallel plates. They studied the effects of viscous dissipation for various values of Darcy number. Siavashi and Rostami[16] also studied laminar heat transfer in partially porous media. In their study, natural convection heat transfer of the non-Newtonian nano fluid, inside an annular pipe with a concentric circular heat source covered with a porous layer are studied numerically. Barnoon and Toghraie[17] investigated the fluid flow and heat transfer of a non-Newtonian nano fluid flowing through a concentric annular pipe partially filled with a porous material. Natural convection of power-law fluids was studied in a wide range of power-law index by kefayati et al.[18] and demonstrated a different manner in comparison with a pure fluid. Mohebi et al. [19] used the LBM method (Lattice Boltzmann method) to examine the flow and convection heat transfer of a non-Newtonian fluid between two parallel plates partially filled with a porous material. They found that pseudo plastic fluid has the highest heat transfer rate compared to Newtonian and Dilatant fluids.

As already mentioned, a few research works have investigated turbulent forced convection of non- Newtonian fluid in ducts or tubes partially filled with porous media. In most researches the non-Newtonian fluid flow regime is considered to be laminar inside a porous layer [7]. In the present study, the forced convection heat transfer of a turbulent flow of a non-Newtonian fluid in an annular pipe containing

porous discs is studied numerically for Reynolds number range of (10000≤Re≤35000). Forchheimer-extended Darcy and local thermal equilibrium equations are utilized to simulate fluid flow and heat transfer in porous discs. The non-Newtonian fluid is modeled with power- law model.

The statement of the problem is presented in the section 2 of the present study. Boundary conditions, momentum and energy equations are presented in both porous region and clear region and also, thermo-physical properties of the working fluid and porous matrix are presented. In the section 3, the grid generation of the research geometry is presented and the validations of the problem of the present study with the experimental results and numerical results are studied. In addition, in the part related to numerical results, the effects of power law index of non-Newtonian fluid, porous disc pitch and porous layer thickness on the amount of heat transfer, friction coefficient and thermal efficiency are presented in the form of diagrams. In the section 4, the results of the present study are mentioned briefly and suggestions for further study are presented.

PROBLEM STATEMENT AND GOVERNING EQUATIONS

As mentioned before, the partially porous media is used in the industry due to its unique properties such as high thermal conductivity of porous matrix and causing channeling effect which increases the heat transfer. As the decreasing the cost of producing heat exchangers is a significant factor in the industry, it is attempted to find a way for increasing the heat transfer which economizes the costs. Therefore the partially porous media are used as porous discs or porous fins which are placed on the outer tube of the annular pipe.

The geometry of the intended problem is an annular pipe containing two concentric pipes with the length of L and inner and outer radius of R_i and R_o, respectively. The number of 6porous aluminum discs with the porosity of φ = 0.9 and thickness and pitch of δ_p and s_p, respectively, are attached to the inner surface of the outer pipe. The schematic of the problem can be seen in figure 1 and 2.

The incompressible and steady state flow of Non-Newtonian fluid enters the space between the two pipes with uniform velocity uin and uniform temperatureTin. The thermophysical properties of the porous matrix and the fluid are assumed to be constant. The porous medium is homogenous and isotropic and is in thermal equilibrium with the fluid. The length of the annular pipe after the last porous discis long enough so that the fully developed condition is provided. In figure 1, R_p is the radius of the porous/fluid interface and S is the non-dimensional porous layer area (cross-section of porous disc coverage) given by:

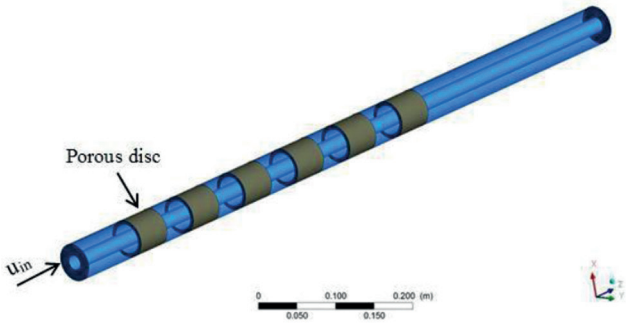

Figure 2. 3D schematic of current problem.

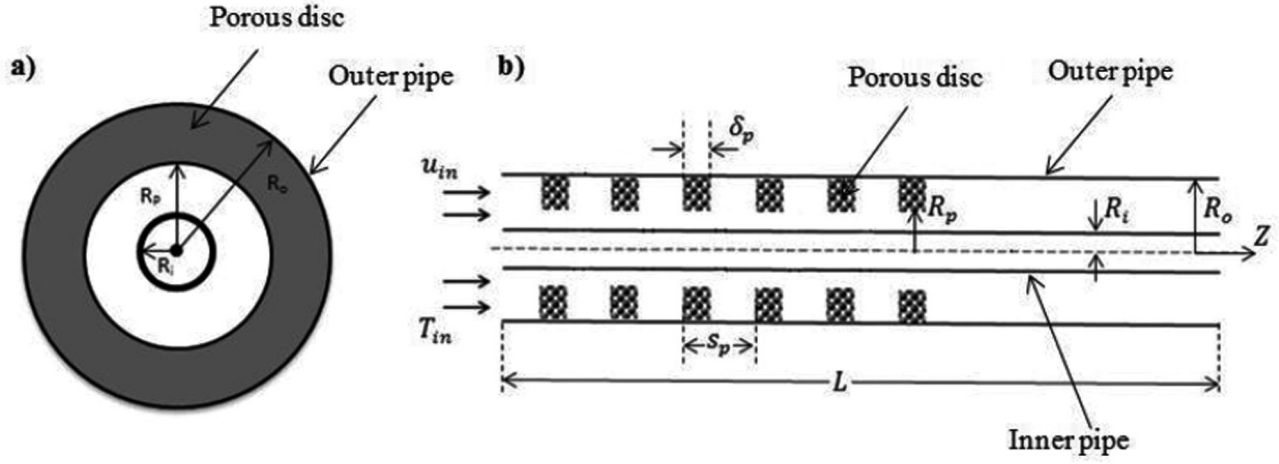

Figure 1. Schematic of the studied geometry (a): cross section of the annular pipe in the porous region (b): longitudinal section.

Table 1. The characteristics of ∇ operator

Operation	Cylindrical Coordinates (r, θ, z)
A vector field	$A_r\hat{r} + A_\theta\hat{\theta} + A_z\hat{z}$
Gradient ∇j	$\frac{\partial j}{\partial r}\hat{r} + \frac{1\partial j}{r\partial,}\hat{\theta} + \frac{\partial j}{\partial z}\hat{z}$
Divergence ∇. A	$\frac{1\partial}{r\partial r}(rA_r) + \frac{1\partial A_,}{r\partial,} + \frac{\partial A_z}{\partial z}$
Laplace operator $\nabla^2 j$	$\nabla^2 - \frac{1\partial}{r\partial r}\left(r\frac{\partial j}{\partial r}\right) + \frac{1\partial^2 j}{r^2\partial,^2} + \frac{\partial^2 j}{\partial z^2}$
Vector Laplacian$\nabla^2 A$	$\left(\nabla^2 A_r - \frac{A_r}{r^2} - \frac{2}{r^2}\frac{\partial A_,}{\partial,}\right)\hat{r} + \left(\nabla^2 A_, - \frac{A_,}{r^2} - \frac{2}{r^2}\frac{\partial A_r}{\partial,}\right)\hat{,} + \nabla^2 A_z\hat{z}$

$$S=\frac{A_p}{A}=\frac{R_o^2-R_p^2}{R_o^2-R_i^2} \quad (1)$$

GOVERNING EQUATIONS IN CLEAR REGION

Firstly, the definitions of different operators in cylindrical coordinate system used in the governing equations are presented in Table1.

The continuity equation in the cylindrical coordinate system is given by[20]:

$$\nabla.\bar{u}=\frac{1\partial}{r\partial r}(ru_r)+\frac{1\partial u,}{r\partial,}+\frac{\partial u_z}{\partial z}=0 \quad (2)$$

The momentum equations for the velocity vector $u(u_r + u_\theta\hat{\theta} + u_z\hat{z})$ in the cylindrical coordinate system are as follows[20]:

$$\rho\nabla.(\bar{u}) = -\nabla P+\mu\nabla^2 u+\nabla.(-\rho\bar{u}) \quad (3)$$

Also the energy equations in the cylindrical coordinate system are as follows[20]:

$$(\rho C_p)\nabla.(\bar{u}T)=\nabla.[\lambda_f.\nabla T] \quad (4)$$

Equations (2) to (4) are solved using the finite volume method. The SIMPLE algorithm is used to handle pressure and velocity coupling. Also the standard k – ε modelthat yields acceptable results for confined flows is used in the present study to consider turbulent fluctuations [21–23].

Turbulent kinetic energy and its dissipation rate equations in standard k – ε model are given by[21]:

$$\rho\nabla.(\bar{u}k)=\nabla.\left[\left(\mu+\frac{\mu t}{\sigma_k}\right)\nabla(k)\right]+P_k-\rho\varepsilon \quad (5)$$

$$\rho\nabla.(\bar{u}\varepsilon)=\nabla.\left[\left(\mu+\frac{\mu t}{\sigma_\varepsilon}\right)\nabla(\varepsilon)\right]+c\,P_1\frac{s}{k_k}-c\,\rho_2\frac{s^2}{k} \quad (6)$$

The P_k in the above equations is the turbulent kinetic energy production rate due to the average velocity gradient.

GOVERNING EQUATIONS IN POROUS REGION

The importance of turbulence inside porous media has been investigated through comparison of turbulent results with those predicted by the laminar model in different Darcy numbers and porous layer thicknesses by Jouybari et al. It is shown that turbulence effects in porous media significantly affect the heat transfer process in composite porous/fluid domain so that, they cannot be neglected even for $R_p < R_{p.critical}$ [24, 25]. Various methods have been proposed by researchers to model the turbulent flow within porous media [26, 27]. Nakayama and Kuwahara[28] developed another k – ε macroscopic model by volume averaging the Navier-Stokes equations over a REV. The possibility of modeling small eddies inside pores was addressed in their method and their equations are as follow:

$$\nabla.\bar{u}_D=0 \quad (7)$$

In which the Dupuit-Forchheimerequation, $\bar{u}_D=\varphi\langle\bar{u}\rangle^i$, was used and $\langle\bar{u}\rangle^i$ states the intrinsic average of the local time-averaged velocity vector $\bar{u}$. The above equation is the macroscopic continuity equation of an incompressible fluid in a rigid porous medium. The Navier-Stokes equations for

steady state turbulent flow of an incompressible fluid with constant properties can be written as follows:

$$\rho\nabla.\left(\frac{\bar{u}_D.\bar{u}_D}{\varphi}\right)=-\nabla\left(\varphi\langle\bar{u}\rangle^i\right)+\mu\nabla^2u_D+\nabla.\left(-\rho\varphi\langle\bar{u}\rangle^i\right)-\left[\frac{\mu\varphi\bar{u}_D}{K}+\frac{C_F\varphi\rho|\bar{u}_D|\bar{u}_D}{\sqrt{K}}\right] \quad (8)$$

In above equation, μ is fluid dynamic viscosity, K and C_F are the porous media permeability and inertia coefficient for Newtonian fluid respectively. Also $-\rho\varphi\langle\bar{u}\rangle^i$ is Reynolds stress tensor defined as:

$$-\rho\varphi\langle\bar{u}\rangle^i=\mu_{t\varphi}2\langle D\rangle^{\vartheta}-\frac{2}{3}\varphi\rho\langle k\rangle^i I \quad (9)$$

In equation (9), $\langle D\rangle^{\vartheta}$ is the macroscopic deformation tensor, $\langle k\rangle^{\vartheta}$ is the intrinsic average of k, and $\mu_{t\varphi}$ is the macroscopic turbulent viscosity which can be modeled as follows[29]:

$$\mu_{t\varphi}=\rho C_\mu\langle k\rangle^i/\langle\varepsilon\rangle^i \quad (10)$$

The macroscopic transport equations for the turbulent kinetic energy and dissipation rate in the porousmedium are as follow[28, 30]:

$$\nabla.\left(\bar{u}_D\langle k\rangle^i\right)=\nabla.\left[\left(\mu+\frac{\mu_{t\varphi}}{\sigma_k}\right)\nabla\left(\sigma\langle k\rangle^i\right)\right]+P_k^i+G_k^i-\rho\sigma\langle\varepsilon\rangle^i \quad (11)$$

$$\nabla.\left(\bar{u}_D\langle\varepsilon\rangle^i\right)=\nabla.\left[\left(\mu+\frac{\mu_{t\varphi}}{\sigma_e}\right)\nabla\left(\varphi\langle\varepsilon\rangle^i\right)\right]+c_1P_k^i\frac{\langle s\rangle^i}{\langle k\rangle^i}+c_2\left(G_s^i-\rho\varphi\frac{\langle s\rangle^i}{\langle k\rangle^i}\right) \quad (12)$$

Where $P_k^i=-\rho\varphi\langle\bar{u}\rangle^i:\nabla.\bar{u}_D$ is the production rate of $\langle k\rangle^i$ due to the velocity gradient of $\bar{u}_D$. The macroscopic turbulence equations in the porous medium have two extra terms which are G_k^i and G_s^i denoting the internal production of turbulent kinetic energy and its dissipation rate due to presence of the solid matrix, respectively[28]. These two terms can be neglected whenever the porosity and permeability of the porous medium are high enough[31, 32]

In order to model the energy transport equation, the LTE (Local Thermal Equilibrium between fluid and solid matrix) assumption has been used. Hence energy equation can be written as follows:

(13)

At the inlet:

$$T=T_{in}=300K \text{ at } (z=0) \quad (14)$$

$$u=u_{in} \text{ at } (z=0) \quad (15)$$

At the outlet:

$$P_{out}=P_{Gauge\ pressure}=0 \text{ at } z=L \quad (16)$$

At the annular walls:

$$u=0 \text{ at } r=R_i \text{ (outer surface of inner pipe)} \quad (17)$$

$$u=0 \text{ at } r=R_o \text{ (inner surface of outer pipe)} \quad (18)$$

$$T=T_w(z)=500K \text{ at } r=R_i \quad (19)$$

$$\frac{\partial T}{\partial r}=0 \text{ at } r=R_o \quad (20)$$

All the equations presented for porous media region (section 3.2), reduce to the clear fluid condition as the porous matrix disappears for φ = 1and $K^{**}\to\infty$. Therefore, the single domain approach can be used to solve fluid/porous interface problems by appropriately changing the properties of the porous medium in the computational domain. Notably, this approach has been thoroughly tested by several groups of researchers [33–35]. It has been shown that the numerical solutions automatically satisfy the continuity of velocities, shear stresses and fluxes across the fluid/porous interface without an additional iterative procedure to match the interface conditions as described in Ref. [33].

In equation (13), λ_{eff} is the effective thermal conductivity which can be obtained through the Calmidi and Mahajan[36] equation for high thermal conductivity of metal foams as follows:

$$\lambda_{eff}=\left[\varphi\lambda_f+0.195(1-\varphi)^{0.763}\lambda_s+\varphi C_{P_f}\frac{\mu_{t\varphi}}{\sigma_T}\right]I \quad (21)$$

The effective thermal conductivity for $\frac{\lambda_s}{\lambda_f}=1$ is defines as:

$$\lambda_{eff}=\left[\varphi\lambda_f+(1-\varphi)\lambda_s+\varphi C_{P_f}\frac{\mu_{t\varphi}}{\sigma_T}\right]I \quad (22)$$

In the above equations, C_μ, C_1, C_2, σ_k, σ_s and σ_T are constant and can be written as follows[27]:

Table 2.properties of the studied fluid

Parameter	Value
$\eta(Pa\ s^n)$	0.001
n	0.6–1.2
$\rho(\frac{kg}{m^3})$	998.2
$Cp(\frac{J}{kg.K})$	4180
$\lambda(\frac{W}{m.K})$	0.6
Minimum viscosity limit	0.0001
Maximum viscosity limit	1000

Table 3. properties of the Al foam

Foam material	$\lambda_{s(aluminum)}\left(\frac{W}{mK}\right)$	φ	$K^{**}(m^2)$
Al foam	218	0.9	$1.2*10^{-7}$

$$C_\mu = 0.09,\ C_1 = 1.44,\ C_2 = 1.92,\quad \sigma_k = 1.0,\ \sigma_s = 1.3,\ \sigma_T = 0.9 \tag{23}$$

NON-NEWTONIAN FLUID

The fluid studied in the present study is non-Newtonian. Thermal characterization of non-Newtonian fluids flow through porous media is a topic of practical engineering importance. The understanding of the heat transfer involved in such flows can have immediate effects on many industrial applications such as those related to oil recovery aided by thermal methods, packed bed reactors, biomechanics where fluids flow through lungs and arteries,pharmaceuticals, filtration, and fixed bed regeneration.

There is not a linear relationship between the shear stress and shear rate in non-Newtonian fluids. Various models have been proposed for non-Newtonian fluids where the most common is the power-law fluid. To show the apparent viscosity of the fluid the power-law model is used[37]. The rheological equation of the non-Newtonian fluidthat shows the relationship between the shear stress and shear rate is given by:

$$\mu_{app} = \eta\dot{\gamma}^{n-1} \tag{24}$$

Where η is the consistency index, n is the flow behavior index, and $\dot{\gamma}$ is the shear rate of the non-Newtonian fluid. When n > 1 the fluid is called Dilatant or shear thickening, when n < 1 the fluid is called pseudo plastic or shear thinning and when n = 1, it is called Newtonian fluid[38].

Simulations were performed for Newtonian and non-Newtonian fluid with the characteristics of table 2:[39]

As mentioned, porous foam material is made from aluminum. Some of the properties of Al foam are as follows:

The inertia coefficient, C* and Permeability, K* for a non-Newtonian fluid can be obtained through theKozeny-Carman equation [40].

$$C^* = C\left(K^*\right)^{-1}/K^{-1} \tag{25}$$

$$K = \frac{d_p{}^2\varphi^3}{150\left(1-\varphi\right)^2} \tag{26}$$

K* is also obtained as follows[41]:

$$K^* = \frac{1}{2c_t}\left(\frac{n\varphi}{3n+1}\right)^n\left(\frac{50K}{3\varphi}\right)^{(n+1)/2} \tag{27}$$

$$c_t = 2.5^n \times 2\left(\frac{1-n}{2}\right) \tag{28}$$

The Reynolds and Darcy numbers in the porous medium for a non-Newtonian fluid are obtained as follows[41, 42]:

$$Re_{porous} = \frac{\left(\frac{K}{\varphi}\right)^{\frac{n}{2}}\left(\frac{u}{\varphi}\right)^{2-n}}{\eta} \tag{29}$$

$$D_a = \frac{\left(\frac{K^*}{\varphi^\mu}\right)^{\frac{2}{1+n}}}{D_b{}^2} \tag{30}$$

According to the above equations, the local and average Nusselt numbers are obtained using the following equations:

$$Nu_X = \frac{q''D_h}{\left(T_w - T_m\right)\lambda_{err}} \tag{31}$$

$$Nu_{avg} = \frac{1}{D}\int Nu_x dx \tag{32}$$

$$f_z = -\left(\frac{dp}{dz}\right)\frac{dh}{\rho u^2 m/2} \tag{32}$$

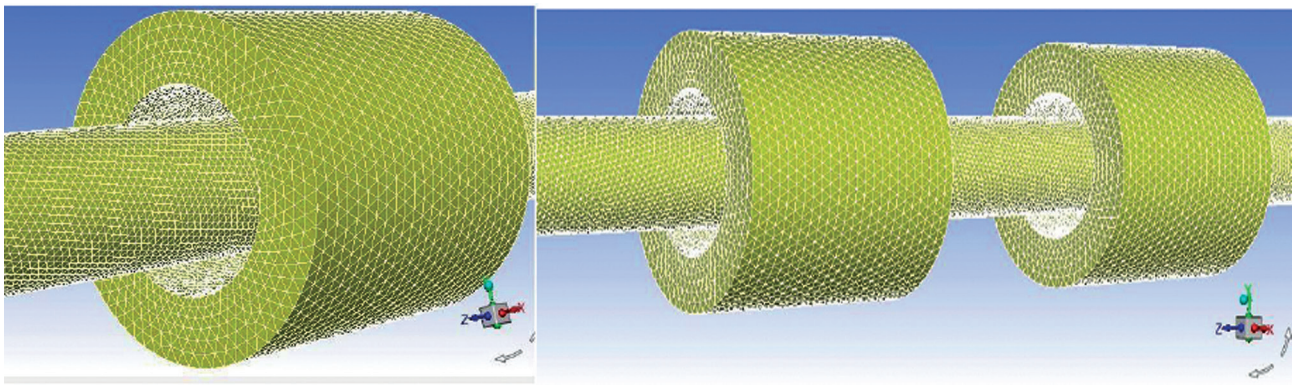

Figure 3. Mesh of the inner tube of the annular pipe and porous discs.

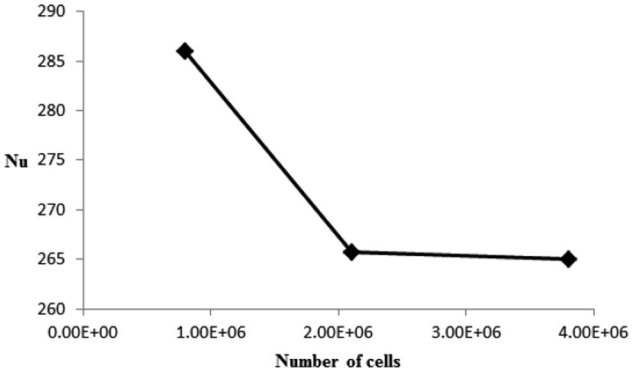

Figure 4. Effect of the number of cells on the Nusselt number on the internal wall of the annular pipe containing porous discs for Da = 10^{-4}, Re = 10000, and S = 0.76.

Table 4. Effect of the number of cells on the Nusselt number on the internal wall of the annular pipe containing porous discs for Da = 10^{-4}, Re = 10000, and S = 0.76

Number of cells	800000	2100000	3800000
Nu	286	265.7	265
Error percent	–	7.6%	0.26%

In the above equations, T_w is the surface temperature of the internal pipe, T_m is the flow average temperature, and D_h is the hydraulic diameter of the annular pipe.

Porous discs prevent fluid to flow freely and consequently increase the pressure drop and the friction coefficient. The local and average friction coefficients are given by[43]:

$$f_z = -\left(\frac{dp}{dz}\right)\frac{dh}{\rho u^2 m/2} \tag{33}$$

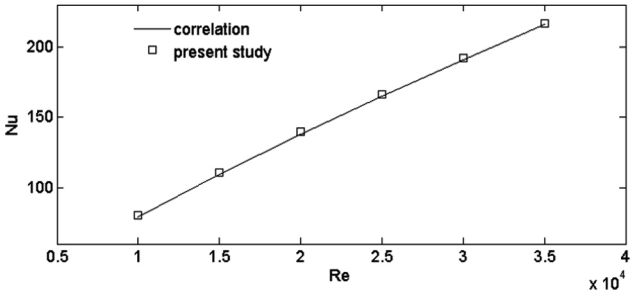

Figure 5. Comparison of the average Nusselt number in the present study against the results of Dittus-Bolter equation.

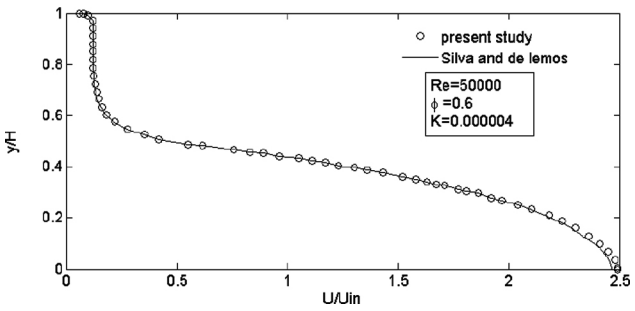

Figure 6. The comparison between the velocity profile obtained in the present study and that of reported by Silva and de Lemos[45].

$$f_z = \frac{1}{D}\int f_z dz \tag{34}$$

To examine the increase in the heat transfer rate versus the pressure loss which occurs in the presence ofporous discs in the annular pipe, one may use the thermal performance coefficient as below[44]:

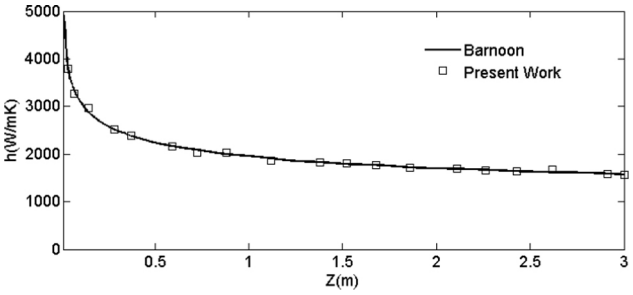

Figure 7. Comparison between the heat transfer coefficients along the pipe length obtained in the present study and Toghraie and Barnoon[17].

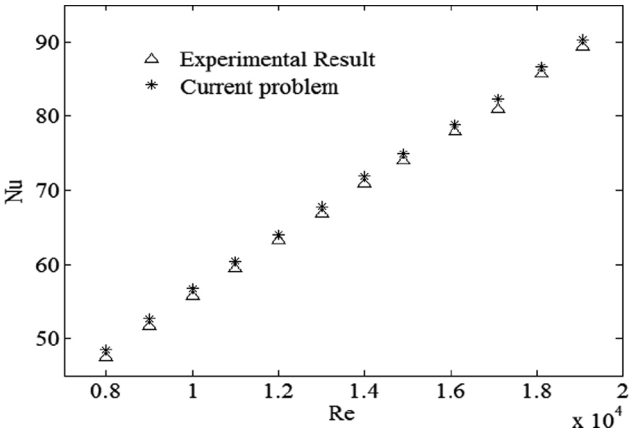

Figure 8. The comparison between Nusselt number obtained in the present study and that of reported by Huang et al. [46].

$$PEC = \frac{Nu/Nu_s}{\left(f/f_s\right)^{1/3}} \quad (35)$$

Where Nu_s and f_s are the Nusselt number and friction coefficient of the non-Newtonian fluid flowing in an empty annular pipe, respectively. Also, Nu and f denote the Nusselt number and friction coefficient of the non- Newtonian fluid flowing in an annular pipe with porous discs, respectively.

GRID INDEPENDENCY AND VALIDATION

The geometry of the research problem is drawn and meshed in three dimensions in the Gambit software that can be seen in figure 3. A 3D-CFD computational model is applied to evaluate non-Newtonian power law fluid flow in the annular pipe filled partially porous media under turbulent regime and steady conditions. The research model is simulated in the Ansys Fluent computational fluid dynamics software using the finite volume method and the flow and energy equations are discretized up to the second order upwind. The value of 10^{-6} is considered as the convergence criterion for all parameters. The annular pipe with porous discs is considered to examine the grid independency of the research geometry and the average Nusselt number of the pseudo plastic non-Newtonian fluid is studied for the mentioned geometry and the values of Da = 10^{-4}, Re = 10000, S = 0.76, and n = 0.85. The results of the grid independency evaluation are demonstrated in figure 4. As can be seen in figure 4 and table 4, the difference between the heat transfer rates for meshing of 2.1×10^6 and 3.8×10^6 is less than 0.5%. Because meshing with more than 2.1×10^6 number of cells does not impose a notable change in the Nusselt number. Thus, this mesh was selected for the numerical solution of all cases.

To validate the porous medium simulation, the obtained results were compared to the velocity profile reported by Silva and de Lemos[45]. Silva and de Lemos[45] studied the turbulent flow with Reynolds of Re = 50000 in a channel partially filled with porous materials (the porous medium

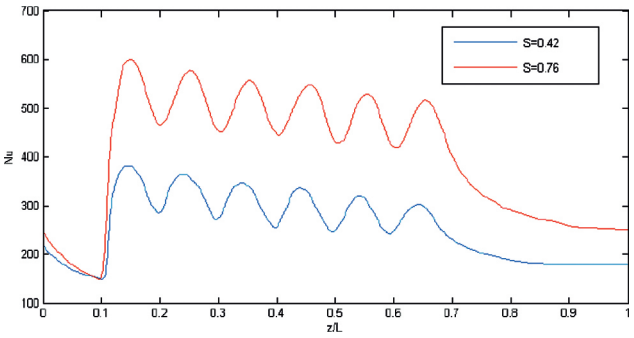

Figure 9. Variation of local Nusselt number along the annular pipe length for Re = 25000, Da = 10^{-4}, n = 0.6, s_p = 0.1.

was attached to the channel's wall in their study). They considered the permeability to be 0.000004, porosity, 0.6, and the dimensionless thickness of the porous layer, 0.5. The velocity profile of the current study is compared with that of Silva and de Lemosin figure 6and they show a good agreement.

For more validation, the results of Toghraie and Barnoon[17]have been utilized to verify the simulation of non-Newtonian fluid flow in porous media in the present study. They used the non-Newtonian nano fluid of CMC + Al_2O_3 which flows through a concentric annular pipe partially filled with porous medium. As shown in figure 7, the results obtained in the present study are in good agreement with the results of Ref.[17].

In addition the experimental results of Huang et al. [46] have been utilized to verify the simulation fluidflow in partially porous media in the present study. They studied the turbulent flow in a tube partially filled with porous materials. In their study, to partially fill the tube with porous

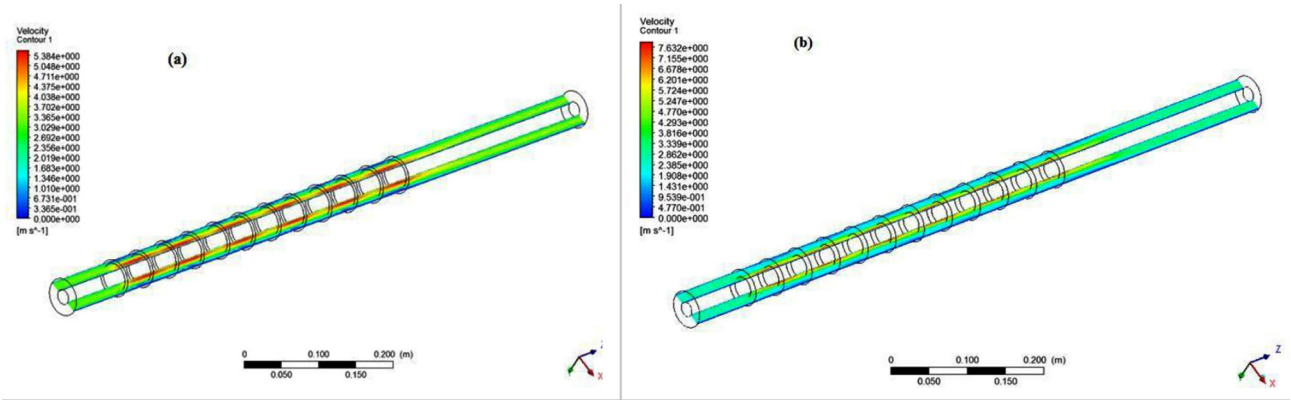

Figure 10. The velocity contour along the annular pipe (y = 0), a)S = 0.42, b) S = 0.76.

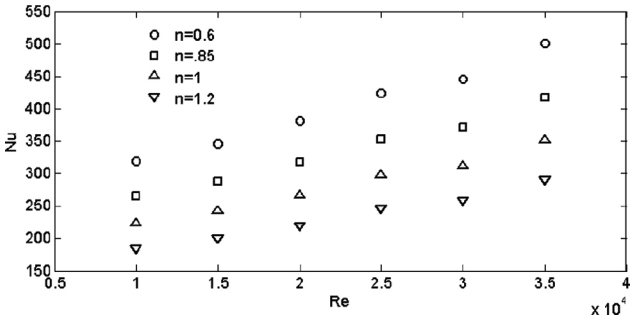

Figure 11. The effect of power-law index on the Nusselt number for different Reynolds numbers for Da = 10^{-4}, S = 0.76, s_p = 0.1.

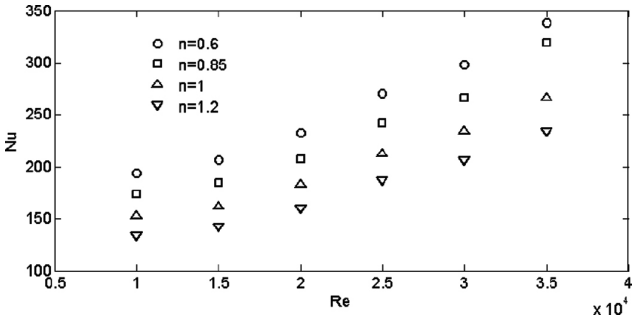

Figure 12. The effect of power-law index on the Nusselt number for different Reynolds numbers for Da = 10^{-4}, S = 0.42, s_p = 0.1.

media, the copper screens at a diameter D_p were located in the core of the tube. They considered the porosity, to be 0.975, and the dimensionless thickness of the porous layer, 0.5. As shown in figure 8, the results obtained in the present study are in good agreement with the results of Huang et al. [46].

RESULTS AND DISCUSSION

In the present study, the non-Newtonian power-law fluid flows between the two concentric pipes of the annular. Porous discs made from Aluminum foam are installed on the inner surface of the outer pipe. In the section 4.1, the effects of porous layer thickness on velocity contour and local Nusselt number is studied. In the part 4.2the effects of the power-law index of non-Newtonian fluid are studied on Nusselt number. By the increase of the amount of heat transfer, the pressure loss increases, so the result related to friction coefficient are presented too. Based on previous studies the thermal performance is the most suitable standard for evaluating the efficiency for the suggested model. Accordingly in this study, in order to determine which model is most suitable to be used in industry, thermal performance coefficient (equation 35) is calculated. In parts 4.3 the effect of the pitch of the porous disc on Nusselt number, friction coefficient and thermal performance is studied.

EFFECT OF POROUS LAYER THICKNESS ON HEAT TRANSFER CHARACTERISTICS

When the fluid with uniform temperature enters the smooth annular pipe the convective heat transfer occurs and the thermal boundary layer starts growing which decreases the convective heat transfer coefficient and the Nusselt number until reaching a fixed value[7, 9]. But results for the annular pipe containing porous discs are different. The local heat transfer rate on inner tube of the annular inner pipe containing porous discs in two cases of S = 0.42 and S = 0.76 can be seen in figure 9.In these cases, decreasing in Nusselt number continues until the first porous disc. At the location of the first porous disc, the Nusselt number surges suddenly. The reason for this sudden rise is that the flow region becomes narrow at porous discs regions and this creates acceleration in the fluid near the porous discs

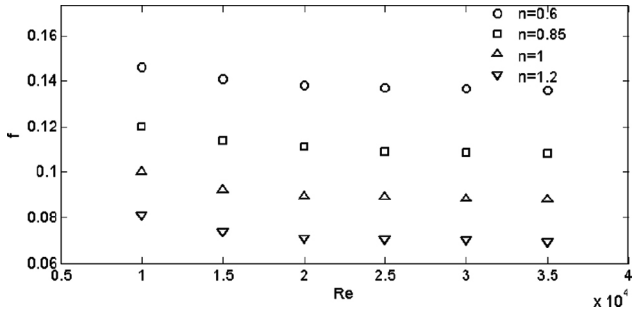

Figure 13. The effect of power-law index on the friction factor for different Reynolds numbers for Da = 10^{-4}, S = 0.76, s_p = 0.1.

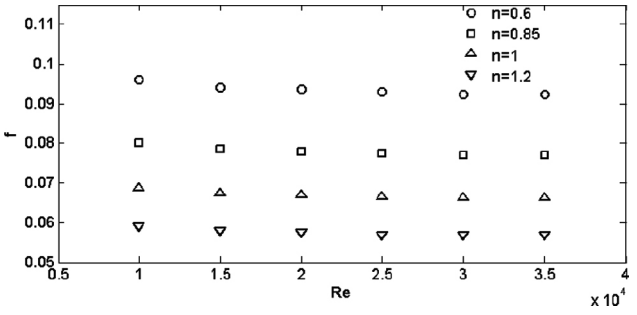

Figure 14. The effect of power-law index on the friction factor for different Reynolds numbers for Da = 10^{-4}, S = 0.42, s_p = 0.1.

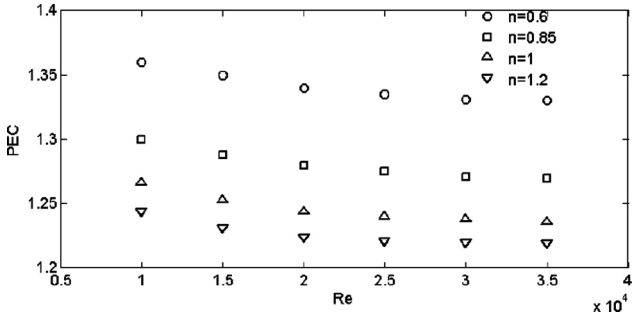

Figure 15. The effect of power-law index on the thermal performance for different Reynolds numbers for Da = 10^{-4}, S = 0.42.

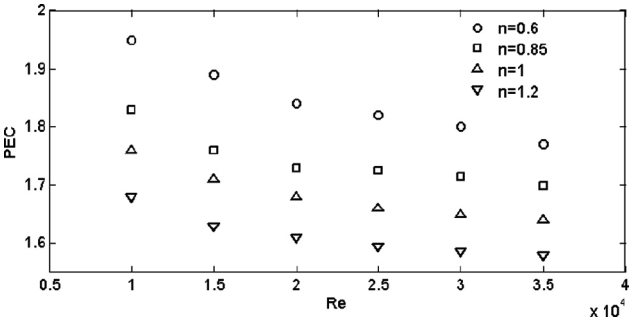

Figure 16. The effect of power-law index on the thermal performance for different Reynolds numbers in Da = 10^{-4}, S = 0.76.

which finally leads to a sudden increase in the heat transfer rate. The maximum value of the local Nu corresponds approximately to the end of the porous disc. The Nusselt number is then gradually decreased after the porous discs(The presence of 6 peaks in the diagram indicates this number of porous discs)[31]. The velocity contour at a cross-section of the pipe (y = 0) is shown in figure 10. The increase in the porous layer cross section area imposes more force on the fluid so that the fluid escapes the porous layer with the greater resistance to the clear region and lower pressure drop. This causes a greater velocity gradient at the inner pipe surface and an increase in the heat transfer rate. Thus, it can be concluded that the Nusselt number increases by the increase in the cross- section of the porous disc coverage from S = 0.42 to S = 0.76 (figure 9)[11].

EFFECT OF POWER-LAW FLUID ON HEAT TRANSFER CHARACTERISTICS

Figure 11 and 12show the Nusselt number versus different indexes of power-law fluid for S = 0.76 and S = 0.42 respectively. As can be observed in Figure 11 and 12, the heat transfer is increased by the increase of the Reynolds number. The heat transfer rate in a pseudo plastic fluid is greater than that of the Newtonian fluid and the heat transfer rate in a Newtonian fluid is greater than that of the Dilatant fluid. Moreover, increasing the pseudo plastic degree of a fluid (reducing the power-law index from n = 0.85 to n = 0.6) enhances the heat transfer rate. It can be attributed to the fact that the fluid deformation near the porous disc surface has the highest value so the pseudo plastic fluid viscosity is the lowest in this region. Thus, increasing the pseudo plastic degree of a fluid increases the heat transfer rate due to a decrease in its effective viscosity.

The variation of the friction factor versus Reynolds number has been shown in figures13 and 14 for S = 0.76 and S = 0.42 respectively. The friction factor decreases by the increase of the Reynolds number because the turbulent layer decreases by increasing the Reynolds number[47]. The friction factor of a pseudo plastic fluid is greater than that of the Newtonian fluid and the friction coefficient of a Newtonian fluid is greater than that of the Dilatant fluid. Moreover, this friction factor increases

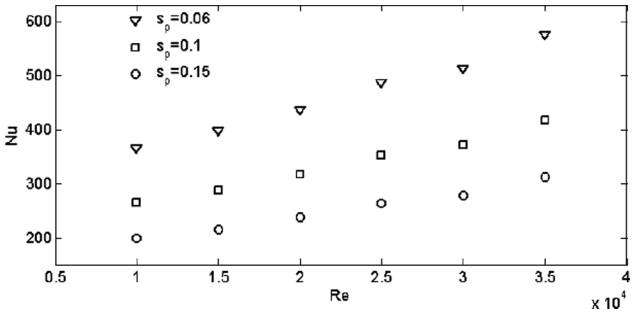

Figure 17. The effect of porous disc pitch on the heat transfer rate at different Reynolds numbers in Da = 10^{-4}, S = 0.76, n = 0.85.

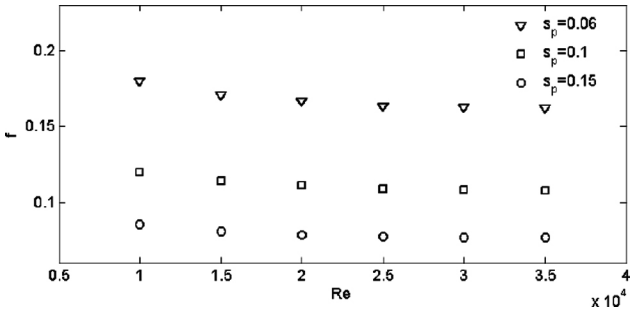

Figure 18. The effect of porous disc pitch on the friction factor at different Reynolds numbers for Da = 10^{-4}, S = 0.76, n = 0.85.

by decreasing the power-law index from n = 0.85 to n = 0.6. Because in the lower value of power-law index more wakes appear behind each porous disc so the friction factor increases. In addition from the comparison of figures 13 and 14, concluded that by increasing S from S = 0.42 to S = 0.76 the space for the fluid flow decreases and the fluid experiences a high resistance, consequently friction factor increases.

The thermal performance versus different indexes of power-law fluid in S = 0.42 can be seen in figure 15. Generally, the thermal performance decreases by the increase in the Reynolds number. This is because the pressure loss increases when the Reynolds number and the flow turbulence are increased. The thermal performance is greater than the unit for all cases. This means that the heat transfer rate is increased high enough to compensate for the increase in the flow resistance and this is an appropriate performance for a heat exchanger. Moreover, the thermal performance of a pseudo plastic fluid or shear thinning is greater than that of the Newtonian and Dilatant fluid. The greatest thermal performance is related to the non-Newtonian fluid with the power-law index of n = 0.6 at Reynolds number of 10000 and it's equal to 1.36. This value is 5% greater than that of a pseudo plastic fluid with a power-law index of n = 0.85 and 8% greater than that of a Dilatant fluid with n = 1.2.

Figure 16 shows the thermal performance of the annular pipe for S = 0.76 and various indexes of non- Newtonian power-law fluid. As can be seen, the thermal performance for the fluid with n = 0.6 and in Re = 10000 is approximately 6% greater than that for the fluid with n = 0.85. Also the thermal performance of power-law fluid with n = 0.6, is 10% greater than that of the Newtonian fluid, and 16% greater than that of the Dilatant fluid. One can conclude from figures 15 and 16 that the thermal performance is considerably increased when the cross-sections of the porous discs coverage increased from S = 0.42 to S = 0.76 and the highest increase is 35-45% where it occurs in a non-Newtonian pseudoplastic fluid.

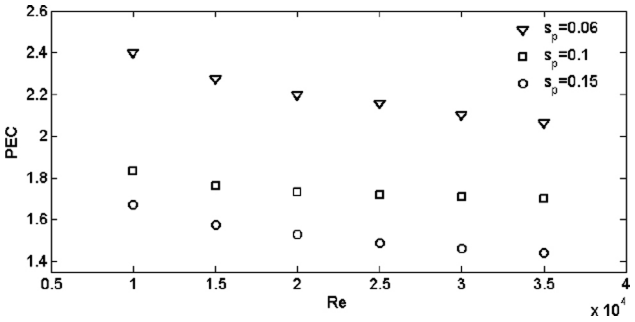

Figure 19. The effect of porous disc pitch on the thermal performance at different Reynolds numbers for Da = 10^{-4}, S = 0.76, n = 0.85.

EFFECT OF POROUS DISCS PITCHES ON HEAT TRANSFER CHARACTERISTICS

A mentioned, channeling effect is occurred due to partially porous media as a result, heat transfer increases. In addition, partially porous media causes increase in the costs because instead of filling all the empty space within the duct, it fills just a part of it. The mechanism of the effects of the partially porous media as porous discs on the amount of heat transfer is explained, in the section4.1. The results showed that the presence of the partially porous media as porous discs cause increase in the velocity of fluid in the location of porous discs and accordingly the increase in the amount of heat transfer. In this section, the effects of porous discs pitches in three cases (s_p = 0.06, 0.1, 0.15) on the amount of heat transfer, friction factor and thermal performance are studied and finally the pitch in which the thermal performance has the highest amount is opted as the most suitable pitch.

Figure 17 shows the Nusselt number versus Reynolds number andfor3 different pitches of the porous discs. Due to the high sensitivity of the convection heat transfer mechanism to the flow turbulence. Applying the porous discs to

the flow path acts as a bump for the stream leads to an interruption for fluid flow and also a disruption for the thermal boundary layer.[48]As the figure reveals, the heat transfer rate for $s_p = 0.06$ is higher than that of $s_p = 0.1, 0.15$. Because the smaller the distance between the discs gets the more discs can be placed in the studied region and consequently, the sudden increase in the local heat transfer rate at porous discs and interruptions in the fluid flow are raised and the average heat transfer rate increases. According to figure 17, the heat transfer rate in an annular pipe containing porous discs and with the pitch of $s_p = 0.06$ is 40% greater than that of the pipe with the pitch of $s_p = 0.1$ and 80% greater than that of the pipe with the pitch of $s_p = 0.15$.

The friction factor coefficient versus the Reynolds number is shown in figure 18 for 3 porous disc pitches. As the figure demonstrates, the friction factor of $s_p = 0.06$ is greater than that of $s_p = 0.1, 0.15$. According to figure 18, the friction coefficient in the annular pipe containing porous disc with the pitch of $s_p = 0.06$ is nearly 50% greater than that of the case with $s_p = 0.1$ and 125% greater than that of the case with$s_p = 0.15$.Reduction of porous discs causes increasing in number of porous discs that create more resistance against fluid flow and consequently pressure drop increases. Figure 19 shows the thermal performance versus the Reynolds number for 3 pitch values of the porous discs. The thermal performance is greater than the unit in all cases which proves that the increase in the heat transfer is high enough to compensate for the increase in the flow resistance. The highest thermal performance is associated with the annular pipe containing porous discs with the pitch of $s_p = 0.06$in Re = 10000, is equal to 2.4.

CONCLUSION AND SUGGESTIONS FOR FUTURE STUDIES

In the present study, the numerical simulation of a turbulent flow of a non-Newtonian fluid in an annular pipe containing porous discs was conducted. The porous discs are placed on the inner tube of the outer pipes in this study.

Studying the effects of porous layer thickness on the amount of heat transfer shows that the main mechanism of increasing the amount of heat transfer in this condition is due to channeling effect in the annular pipe and heat transfer rate increases by the increase in the porous layer thickness.

Furthermore, the results show that reduction of porous discs pitches causes increasing in heat transfer rate. In addition, studies on power-law index of non- Newtonian fluids show that by decreasing the power law index, the amount of heat transfer increases and accordingly the friction coefficient goes up. Therefore the amount of heat transfer and friction coefficient of pseudo-plastic fluid is more than dilatant and Newtonian fluid.

This paper has been mainly focused on the effect of non-Newtonian fluid and porous disc pitch on the heat transfer enhancement. The following ideas could be investigated in the future works:

- Non-Newtonian nano fluids can be used as the working fluid and the effect of different volume concentration of nano fluid can be investigated on the heat transfer rate.
- Porous discs can be inserted adjacent to the outer surface of the inner pipe instead of the inner surface of outer pipe and the effects of these two arrangements can be compared with each other.

NOMENCLATURE

C_p	Specific heat capacity
c_F	Inertia coefficient
Da	Darcy number
D_h	Hydraulic diameter
f	Friction factor
η	Consistency index
K	Turbulent kinetic energy
K	Permeability
K*	Modified permeability
L	Length of the annular
L	length
Nu_x	Local Nusselt number
Nu	Average Nusselt number
P	Pressure
q_w	Heat flux
Re	Reynolds number
R	Radius

Greek

δ	Thickness
ε	Dissipation rate of turbulent energy
λ	Thermal conductivity
μ	Viscosity of fluid
ρ	Density
φ	Porosity

Subscripts

i	inner radius of outer pipe
in	inlet value
m	bulk
o	outer radius of inner pipe
out	outlet value
p	porous
s	smooth tube
t	turbulent
w	wall
R	Radial position measured from centerline
S	Pitch
S	Cross section area
T	Temperature
$\bar{U}$	Velocity vector

AUTHORSHIP CONTRIBUTIONS

Authors equally contributed to this work.

DATA AVAILABILITY STATEMENT

The authors confirm that the data that supports the findings of this study are available within the article. Raw data that support the finding of this study are available from the corresponding author, upon reasonable request.

CONFLICT OF INTEREST

The author declared no potential conflicts of interest with respect to the research, authorship, and/or publication of this article.

ETHICS

There are no ethical issues with the publication of this manuscript.

REFERENCES

[1] Nebbali R, Bouhadef K. Non-Newtonian fluid flow in plane channels: Heat transfer enhancement using porous blocks. Int J Therm Sci 2011;50:1984-1995. [CrossRef]

[2] Bayareh M. Study of the effect of the porous plates on the tank bottom on the boiling process. 2019;5:149-156. [CrossRef]

[3] Mohamad A. Heat transfer enhancements in heat exchangers fitted with porous media Part I: Constant wall temperature. Int J Therm Sci 2003;42:385-395. [CrossRef]

[4] Delavar M, Azimi M. I using porous material for heat transfer enhancement in heat exchangers. J Eng Sci Technol Rev 2013;6:14.

[5] Yacine OA. Computational analysis of inserted porous blocks into horizontal concentric annuli in mixed convection mode. J Therm Eng 2018;4:1692-1701. [CrossRef]

[6] Targui N, Kahalerras H. Analysis of fluid flow and heat transfer in a double pipe heat exchanger with porous structures. Mater Sci 2008;49:3217-3229. [CrossRef]

[7] Yang Y-T, Hwang M-L. Numerical simulation of turbulent fluid flow and heat transfer characteristics in heat exchangers fitted with porous media. Int J Heat Mass Transf 2009;52:2956-2965. [CrossRef]

[8] Allouache N, Chikh S. Numerical modeling of turbulent flow in an annular heat exchanger partly filled with a porous substrate. J Porous Media 2008;11:617-632. [CrossRef]

[9] Nimvari ME, Maerefat M, El-Hossaini M. Numerical simulation of turbulent flow and heat transfer in a channel partially filled with a porous media. Int J Therm Sci 2012;60:131-141. [CrossRef]

[10] Mahmoudi Y, Karimi N. Numerical investigation of heat transfer enhancement in a pipe partially filled with a porous material under local thermal non-equilibrium condition. Int J Heat Mass Transf 2014;68:161-173. [CrossRef]

[11] Jamarani A, Maerefat M, Jouybari NF, Nimvari ME. Thermal performance evaluation of a double-tube heat exchanger partially filled with porous media under turbulent flow regime. Transport in Porous Media 2017;120:449-471. [CrossRef]

[12] Chen G, Hadim H. Forced convection of a power-law fluid in a porous channel–numerical solutions. Heat Mass Transf 1998;34:221-228. [CrossRef]

[13] Nebbali R, Bouhadef K. Numerical study of forced convection in a 3D flow of a non-Newtonian fluid through a porous duct. Int J Numer Methods Heat Fluid Flow 2006;16:870-889. [CrossRef]

[14] Yilmaz N,. Bakhtiyarov AS, Ibragimov RN. Experimental investigation of Newtonian and non-Newtonian fluid flows in porous media. Mech Res Commun 2009;36:638-641. [CrossRef]

[15] Chen G, Tso C. Effects of viscous dissipation on forced convective heat transfer in a channel embedded in a power-law fluid saturated porous medium. Int Commun Heat Mass Transf 2011;38;57-62. [CrossRef]

[16] Siavashi M, Rostami A. Two-phase simulation of non-Newtonian nanofluid natural convection in a circular annulus partially or completely filled with porous media. Int J Mech Sci 2017;133:689-703. [CrossRef]

[17] Barnoon P, Toghraie D. Numerical investigation of laminar flow and heat transfer of non-Newtonian nanofluid within a porous medium. Powder Technol 2018;325:78-91. [CrossRef]

[18] Kefayati GR, Tang H, Chan A, Wang X. A lattice Boltzmann model for thermal non-Newtonian fluid flows through porous media. Comput Fluids 2018;176:226-244. [CrossRef]

[19] Mohebbi R, Delouei AA, Jamali A, Izadi M. and. Mohamad AA. Pore-scale simulation of non-Newtonian power-law fluid flow and forced convection in partially porous media: Thermal lattice Boltzmann method. Phys A Stat Mech Appl 2019;525:642-656. [CrossRef]

[20] Syed KS, Ishaq M, Bakhsh M. Laminar convection in the annulus of a double-pipe with triangular fins. Comput Fluids 2011;44:43-55. [CrossRef]

[21] Ahsan M. Numerical analysis of friction factor for a fully developed turbulent flow using k–ε turbulence model with enhanced wall treatment. Beni-Suef Univ J Basic Appl Sci 2014;3:269-277. [CrossRef]

[22] Ozden E, Tari I. Shell side CFD analysis of a small shell-and-tube heat exchanger. Energy Convers Manag 2010;51:1004-1014. [CrossRef]
[23] Bahmani MH, Sheikhzadeha G, Zarringhalam M, Akbari OA, Alrashedd AAAA, Sheikh Shabani GA, Goodarzie M. Investigation of turbulent heat transfer and nanofluid flow in a double pipe heat exchanger. Adv Powder Technol 2018;29:273-282. [CrossRef]
[24] Jouybari NF, Lundstrom S, Hellstrom JGI, Maerefat M, Nimvari ME. Numerical computation of macroscopic turbulent quantities in a porous medium: an extension to a macroscopic turbulence model. J Porous Media 2016;19:497-513. [CrossRef]
[25] Dybbs A, Edwards R. A new look at porous media fluid mechanics—Darcy to turbulent," in Fundamentals of transport phenomena in porous media. Berlin: Springer, 1984:199-256. [CrossRef]
[26] Antohe B, Lage J. A general two-equation macroscopic turbulence model for incompressible flow in porous media. Int J Heat Mass Transf 1997;40:3013-3024. [CrossRef]
[27] Pedras MH, de Lemos M. Macroscopic turbulence modeling for incompressible flow through undeformable porous media. Int J Heat Mass Transf 2001;44:1081-1093. [CrossRef]
[28] Nakayama A, Kuwahara F. A macroscopic turbulence model for flow in a porous medium. J Fluids Eng 1999;121:427-433. [CrossRef]
[29] De Lemos MJ. Turbulence in porous media: modeling and applications. Amsterdam: Elsevier, 2012. [CrossRef]
[30] Fethallah F. Unsteady numerical simulation of turbulent forced convection in a rectangular pipe provided with waved porous baffles. 2017;3:1466-1477. [CrossRef]
[31] Nazari M, Mohebbi R, Kayhani M. Power-law fluid flow and heat transfer in a channel with a built- in porous square cylinder: Lattice Boltzmann simulation. J Non-Newtonian Fluid Mech 2014;204:38-49. [CrossRef]
[32] Nield D. The limitations of the Brinkman-Forchheimer equation in modeling flow in a saturated porous medium and at an interface. Int J Heat Fluid Flow 1991;12:269-272. [CrossRef]
[33] Chan H-C, Huang W, Leu J-M, Lai C-J, Macroscopic modeling of turbulent flow over a porous medium. Int J Heat Fluid Flow 2007;28:1157-1166. [CrossRef]
[34] Silva RA, De Lemos MJ. Turbulent flow in a composite channel. Int Commun Heat Mass Transf 2011;38:1019-1023. [CrossRef]
[35] Vafai K, Kim S-J. Analysis of surface enhancement by a porous substrate. J Heat Transf 1990;112:700-706. [CrossRef]
[36] Calmidi V, Mahajan R. The effective thermal conductivity of high porosity fibrous metal foams. J Heat Transf 1999;121:466-471. [CrossRef]
[37] Nasiri M, Etemad SG, Bagheri R. Experimental heat transfer of nanofluid through an annular duct. Int Commun Heat Mass Transf 2011;38:958-963. [CrossRef]
[38] Prasad KV, Santhi SR, Datti PS. Non-Newtonian power-law fluid flow and heat transfer over a non-linearly stretching surface. Appl Math 2012;3:425-435. [CrossRef]
[39] Farajzadeh M, Tohidi A. Mixing and heat transfer enhancement of power-law fluids inside helically coiled tube by chaotic advection. J Non-Newtonian Fluid Mech 2019;274:104202. [CrossRef]
[40] Nebbali R, Bouhadef K, Non-Newtonian fluid flow in plane channels: Heat transfer enhancement using porous blocks. Int J Therm Sci 2011;50:1984-1995. [CrossRef]
[41] Shenoy A. Non-Newtonian fluid heat transfer in porous media. Adv Heat Transf 1994;24:101-190. [CrossRef]
[42] Heydari M, Toghraie D, Akbari OA. The effect of semi-attached and offset mid-truncated ribs and Water/TiO2 nanofluid on flow and heat transfer properties in a triangular microchannel. Therm Sci Eng Progress 2017;2:140-150. [CrossRef]
[43] Wu Z, Wang L, Sunden B. Pressure drop and convective heat transfer of water and nanofluids in a double-pipe helical heat exchanger. Appl Therm Eng 2013;60:266-274. [CrossRef]
[44] Da Silva Miranda BM, Anand N. Convective heat transfer in a channel with porous baffles. Numer Heat Transf Part A Appl 2004;46:425-452. [CrossRef]
[45] Silva RA, de Lemos MJ. Turbulent flow in a channel occupied by a porous layer considering the stress jump at the interface. Int J Heat Mass Transf 2003;46:5113-5121. [CrossRef]
[46] Huang Z, Nakayama A, Yang K, Yang C, Liu W. Enhancing heat transfer in the core flow by using porous medium insert in a tube. Int J Heat Mass Transf 2010;53:1164-1174. [CrossRef]
[47] Khanmohammadi F, Farhadi M,. Darzi AAR. Numerical investigation of heat transfer and fluid flow characteristics inside tube with internally star fins. Heat Mass Transf 2018;55:1901-1911. [CrossRef]
[48] Mozafarie SS, Javaherdeh K, Ghanbari O. Numerical simulation of nanofluid turbulent flow in a double-pipe heat exchanger equipped with circular fins. J Therm Anal Calorim 2020;144:1401-1416. [CrossRef]